Molecular Crystals and Liquid Crystals

Publication details, including instructions for authors and subscription information:
http://www.tandfonline.com/loi/gmcl20

Nematic Phases of Disc-And Rod-Shaped Molecules

Paul H. J. Kouwer [a] & Georg H. Mehl [a]

[a] Department of Chemistry, University of Hull, Cottingham Road, Hull, HU6 7RX, United Kingdom

Version of record first published: 18 Oct 2010

To cite this article: Paul H. J. Kouwer & Georg H. Mehl (2003): Nematic Phases of Disc-And Rod-Shaped Molecules, Molecular Crystals and Liquid Crystals, 397:1, 1-16

To link to this article: http://dx.doi.org/10.1080/713738746

Mol. Cryst. Liq. Cryst., Vol. 397, pp. 1/[301]–16/[316], 2003

ISSN: 1542-1406 print/1563-5287 online
DOI: 10.1080/15421400390213618

Taylor & Francis
Taylor & Francis Group

NEMATIC PHASES OF DISC-AND ROD-SHAPED MOLECULES

*Paul H. J. Kouwer and Georg H. Mehl**
University of Hull, Department of Chemistry, Cottingham Road, Hull, HU6 7RX, United Kingdom

Substantial effort has been made to prepare mixtures of disc-shaped and rod-shaped mesogens, since these mixtures provide one of the requirements in one of the routes towards biaxiality in nematic mesophases. We present the synthesis and mesomorphic properties of two novel liquid crystals based on a disc-shaped mesogen and multiple rod-shaped mesogens. The materials show enantiotropic nematic phases and mixing studies point out that the linked disc-rod mesogens are miscible with both the disc-shaped and the rod-shaped precursors.

Keywords: liquid crystals; nematic; discotic; calamitic; mixtures

INTRODUCTION

Twenty-five years of research on discotic liquid crystals [1] has resulted in the synthesis and characterisation of numerous disc-shaped mesogens [2a]. Peculiarly, in all these liquid crystalline materials, the nematic phase is rarely observed [2b], while this phase is commonly found for rod-shaped liquid crystals.

In the nematic phase formed by disc-shaped mesogens, the molecules are aligned with their short axes along the director **n**, see Figure 1a. The observed phase generally shows a negative birefringence, i.e. $\Delta n \equiv n_e - n_o < 0$. In contrast, the nematic phase of rod-shaped (or calamitic) molecules is formed by alignment of the long axes of the mesogen along the director, see Figure 1b. Most of the rod-shaped mesogens (such as the materials in this study) show a positive birefringence, ($\Delta n > 0$).

From theoretical studies, it has been proposed that the nematic biaxial phase may occur in mixtures of disc-shaped and rod-shaped particles [3].

We like to thank the Ramsay Memorial Fellowship Trust and the European Union (contract HPRN-CT2000-00016) for financial support.

*Corresponding author. Fax: +44 1482 466411, E-mail: p.h.j.kouwer@hull.ac.uk, g.h.mehl@hull.ac.uk

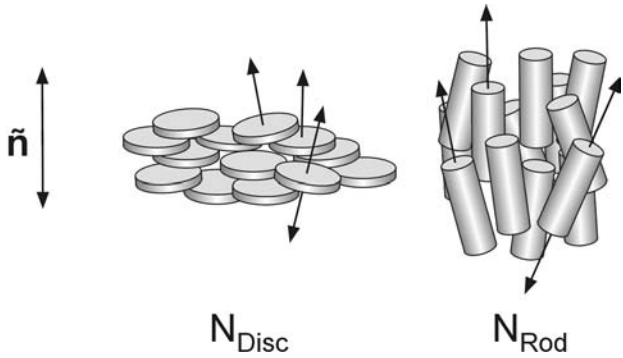

FIGURE 1 Schematic representation of the nematic phase formed by (a) disc-shaped mesogens and (b) rod-shaped mesogens. The arrows indicate the axes of the molecules that align to the director **n**.

One approach is to simply mix discotic and calamitic mesogens in the nematic phase. Although mixing of both moieties in the nematic phase is not prohibited for symmetry reasons (both materials show a uniaxial nematic mesophase), stable mixtures of rods and discs have not been observed so far. In fact, in all studied systems macroscopic phase separation occurs, probably due to the incompatibility of the different shapes of the mesogens and the absence of attractive interactions between the not-alike species [4].

In order to prevent the phase separation process, discs and rods have been linked covalently, where the rod-shaped mesogens have been connected to the disc-shaped moiety via end-on [5a] (see Fig. 2a) or a side-on [5b] (see Fig. 2b) attachment. These materials exhibited monotropic nematic phases only.

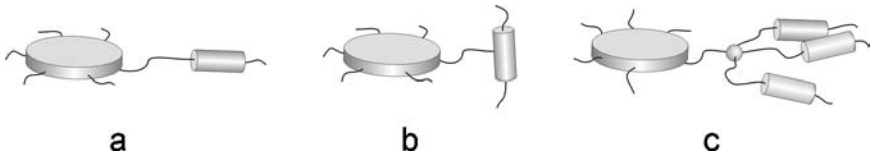

FIGURE 2 Illustration of the considered combinations of covalently linked rod-shaped and disc-shaped mesogens: (a) with the rods end-on attached to the disc [5b]; (b) with the rods side-on attached to the disc [5a] and (c) our current investigations: with multiple rods (linked together in an end-on fashion) attached to a single disc.

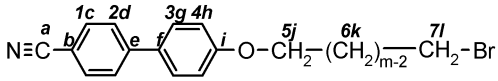

FIGURE 3 NMR assignment for linked cyanobiphenyl mesogens.

In this article, we present two novel mesogens that combine disc-shaped as well as rod-shaped mesogens. In order to obtain similar volume fractions (or weight fractions) of disc- and rod-shaped materials, we linked three rod-shaped species to a single disc [6], see Figure 2c. The synthesis, chemical characterisation as well as the liquid crystalline phase behaviour are presented in this article.

EXPERIMENTAL SECTION

Materials

All materials were used as purchased unless mentioned otherwise. THF has been distilled from sodium prior to use. The synthesis and characterisation of mesogen **D1** has been fully described previously [7].

Instrumental

Nuclear magnetic resonance (NMR) spectra were recorded on a Jeol JNM-ECP 400 FT-IR spectrometer (400 MHz). Chemical shifts are reported in ppm relative to TMS. The ^{1}H-NMR, ^{13}C NMR and ^{19}F NMR data refers to the figures that are shown in the experimental section. In some ^{13}C NMR spectra, multiple peaks are reported for because of the chemical dissimilarity of seemingly equal carbon atoms. The thermal properties were investigated using a Perkin Elmer DSC 7 differential calorimeter (DSC) in nitrogen against an indium standard. Transition temperatures were determined as the onset of the maximum in the endotherm or exotherm. The mesophases were studied on an Olympus BH-2 optical polarising microscope, equipped with a Mettler FP82 HT hot stage and a Mettler FP90 central processor. Pictures of the mesophases were taken with a JVC digital video camera and images were captured with the commercially available "studio capture" software, supplied by studio & designs.

Synthesis

Alkylation of an aromatic alcohol with α,ω-dibromoalkane: A mixture of the 4-cyano-4′-hydroxybiphenyl (**1**, 1 eq.), dibromoalkane (5 eq.), K_2CO_3 (6

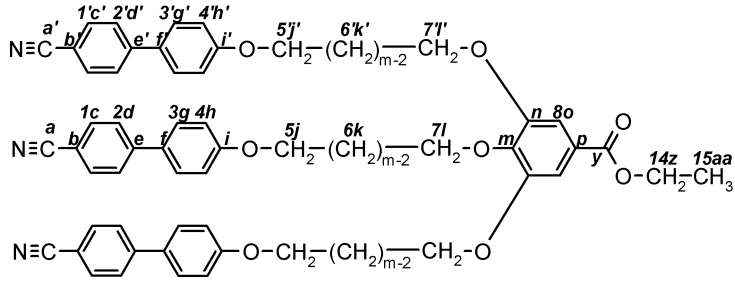

FIGURE 4 NMR assignment for linked cyanobiphenyl mesogens **R1** and **R2**.

eq.), KI (0.5 eq.) and butanone was refluxed overnight. The mixture was allowed to cool to room temperature, the solids were filtered off and the solvent was evaporated under reduced pressure. The oily residue was precipitated in methanol (at least five times the volume) and the crude product was filtered.

4′-(6-Bromohexyloxy)biphenyl-4-carbonitrile (2)

Synthesis according to the general procedure. Purification by two crystallisations from acetone:hexane. Yield: 81% of a white powder. Thermal behaviour: K [N 61°C ($1.7\,J\,g^{-1}$)] 69°C ($73.7\,J\,g^{-1}$) I. ^{1}H NMR (400 MHz, $CDCl_3$): δ 7.66, 7.61, 7.51, 6.97 (4 × dd, 8H, *H1*,*H2*,*H3* and *H4*, resp.); 3.99 (t, 2H, *H5*); 3.40 (t, 2H, *H7*); 1.92–1.78, 1.66–1.57 (2 × m, H6). ^{13}C NMR

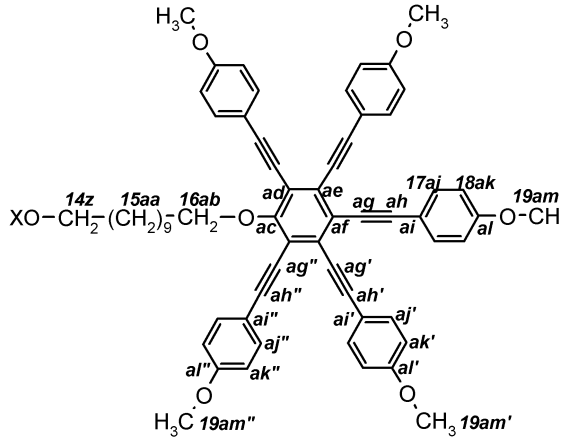

FIGURE 5 NMR assignment for linked disc-rod mesogens **D1R1** and **D1R2**. X represents the gallic acid moiety with the three rod-shaped mesogens attached which are numbered as before (see Figure 4).

(400 MHz, $CDCl_3$): δ 159.64 (*i*); 145.18 (*e*); 132.51 (*c*); 131.28 (*f*); 128.28 (*g*); 127.02 (*d*); 119.06 (*a*); 115.01 (*h*); 109.99 (*b*); 67.83 (*j*); 32.60 (*l*); 33.75, 28.98, 27.85, 25.23 (*k*).

4′-(10-Bromodecyloxy)biphenyl-4-carbonitrile (3)

Synthesis according to the general procedure. Purification by crystallisation from acetone:MeOH and CH_2Cl_2:hexane. Yield: 78% of a white powder. Thermal behaviour: K [N 61°C (1.7 J g^{-1})] 69°C (73.7 J g^{-1}) I. ^{1}H NMR (400 MHz, $CDCl_3$): δ 7.66, 7.61, 7.51, 6.97 (4 × dd, 8H, *H1*, *H2*, *H3* and *H4*, resp.); 3.99 (t, 2H, *H5*); 3.40 (t, 2H, *H7*); 1.92–1.78, 1.66–1.57 (2 × m, H6). ^{13}C NMR (400 MHz, $CDCl_3$): δ 159.64 (*i*); 145.18 (*e*); 132.51 (*c*); 131.28 (*f*); 128.28 (*g*); 127.02 (*d*); 119.06 (*a*); 115.01 (*h*); 109.99 (*b*); 67.83 (*j*); 32.60 (*l*); 33.75, 28.98, 27.85, 25.23 (*k*).

Alkylation of ethyl gallate to prepare the linked rod-shaped mesogens: A mixture of ethyl gallate (1 eq.), ω-bromoalkyl-substituted cyanobiphenyl (4 eq.), K_2CO_3 (6 eq.), KI (0.5 eq.) and butanone was refluxed overnight. The mixture was allowed to cool to room temperature, the solids were filtered off, washed thoroughly with warm acetone or toluene and the solvent was evaporated under reduced pressure. The residue was diluted with some CH_2Cl_2 and precipitated in methanol (at least five times the volume) and the product (and excess starting material) was filtered.

3,4,5-Tris[6-(4′-cyanobiphenyl-4-yloxy)hexyloxy]benzoic acid ethyl ester (R1)

Synthesis according to the general procedure. Purification using column chromatography (SiO_2, eluent CH_2Cl_2:hexane (1:1) to CH_2Cl_2). Yield: 81% of a white powder. ^{1}H NMR (400 MHz, $CDCl_3$): δ 7.68–7.57 and 7.53–7.45 (2 × m, 18H, *H1–H3*); 7.27 (s, 2H, *H8*); 6.97–6.92 (m, 6H, *H4*); 4.35 (q, 2H, *H14*); 4.04, 4.03, 3.99 and 3.97 (4 × t, 12H, *H7* and *H5*); 1.91–1.73 and 1.64–1.50 (2 × m, 24H, *H6*); 1.38 (t, 3H, *H15*). ^{13}C NMR (400 MHz, $CDCl_3$): δ 166.35 (*y*); 159.66 (*i*); 152.68 (*n*); 145.14, 145.09 (*e*); 142.05 (*m*); 132.51 (*c*); 131.25, 131.22 (*f*); 128.28, 128.25 (*g*); 126.99, 126.98 (*d*); 125.21 (*p*); 119.05, 119.02 (*a*); 115.01, 114.98 (*h*); 110.02 (*b*); 107.93 (*o*); 73.20 (*l*); 68.92 (*l′*); 67.99, 67.91 (*j*); 61.02 (*z*); 30.19, 29.22, 29.19, 29.16, 25.89, 25.85, 25.79 (*k*); 14.38 (*aa*).

3,4,5-Tris[10-(4′-cyanobiphenyl-4-yloxy)decyloxy]benzoic acid ethyl ester (R2)

Synthesis according to the general procedure. Purification by crystallisation from MeOH:CH_2Cl_2 and acetone. Yield: 96% of a white powder. ^{1}H NMR (400 MHz, $CDCl_3$): δ 7.68–7.58 and 7.52–7.45 (2 × m, 18H, *H1–H3*); 7.24 (s, 2H, *H8*); 6.98–6.94 (m, 6H, *H4*); 4.33 (q, 2H, *H14*); 4.02,

4.01, 3.97 and 3.96 (4 × t, 12H, ***H7*** and ***H5***); 1.91–1.25 (m, 48H, ***H6***); 1.37 (t, 3H, ***H15***). ^{13}C NMR (400 MHz, $CDCl_3$): δ 166.44 (*y*); 159.75 (*i*); 152.74 (*n*); 145.22, 145.19 (*e*); 142.18 (*m*); 132.53 (*c*); 131.22 (*f*); 128.27 (*g*); 127.02 (*d*); 125.07 (*p*); 119.08 (*a*); 115.03 (*h*); 110.01 (*b*); 107.91 (*o*); 73.40 (*l*); 69.10 (*l′*); 68.10 (*j*); 60.98 (*z*); 30.28–25.99 (*k*), 14.39 (*aa*).

Esterification reaction to prepare the linked disc-rod mesogens: The free carboxylic acids of the linked rod-shaped mesogens **R1** and **R2** were prepared by refluxing the corresponding ethyl esters in ethanol (50 ml) and aqueous KOH (5 ml, 4N). The solution was refluxed until TLC indicated complete consumption of the starting material. The reaction mixture was neutralised with conc. HCl, cooled and the precipitated product was filtered from the mixture. Due to the very low solubility of these mesogens, they were not further isolated, but the products were directly used for the esterification with the disc-shaped mesogens.

A mixture of the gallic acid (with two or three linked rod-shaped mesogens) (1 eq.) and the disc-shaped mesogen (1 eq., ca. 100–200 μmol), dicyclohexylcarbodiimide (DCC, 10 eq.), dimethylaminopyridine (DMAP, 0.5 eq.) and *para*-toluene sulphonic acid (*p*TSA, 0.5 eq.) in CH_2Cl_2 or THF (5–10 ml) was stirred for 3–8 days at room temperature under inert atmosphere. Then the solvent was removed under reduced pressure, the residue was diluted with the eluent and the mixture was directly applied to a column for chromatography. Pure samples were obtained after further chromatography and/or recrystallisations.

3,4,5-Tris[6-(4′-cyanobiphenyl-4-yloxy)hexyloxy]benzoic acid 11-[pentakis(4-hexyloxyphenyletynyl)phenoxy] undecyl ester (D1R1)

Synthesis according to the general procedure. Purification using column chromatography (SiO_2, eluent EtOAc:hexane (3:2)) and recrystallisation from MeOH:CH_2Cl_2. Yield: 41% of a pale yellow powder. ^{1}H NMR (400 MHz, $CDCl_3$): δ 7.65–7.39 (m, 28H, ***H1-3*** and ***H17***); 7.25 (s, 2H, ***H8***); 6.88–6.75 (m, 16H, ***H4*** and ***H18***); 4.30 (t, 2H, ***H14***); 4.27 (t, 2H, ***H16***); 4.01 (t, 12H, ***H7***) 3.98–3.91 (m, 16H, ***H5*** and ***H19***); 1.92–1.25 (m, 82H, ***H6***, ***H15*** and ***H20***); 0.85–0.94 (m, 15H, ***H21***). ^{13}C NMR (400 MHz, $CDCl_3$): δ 166.38 (*y*); 159.85 (*ac*); 159.66, 159.51, 159.45 (*al*); 159.63 (*i*); 152.69 (*n*); 145.14, 145.09 (*e*); 142.06 (*m*); 133.24, 133.10, 133.06 (*aj*); 132.51 (*c*); 131.19 (*f*); 128.37 (*ac*); 128.26 (*g*); 126.98 (*d*); 125.25 (*p*); 123.87 (*af*); 119.80 (*ad*); 119.06, 119.02 (*a*); 115.21, 115.14, 115.10 (*ai*); 114.98 (*h*); 114.61, 114.59, 114.58 (*ak*); 110.02, 109.97 (*b*); 107.92 (*o*); 99.31, 99.08, 97.08 (*ag*); 86.60, 86.06, 83.55 (*ah*); 74.55 (*z*); 73.22 (*l*); 68.94 (*l′*); 68.09 (*am*); 67.99, 67.90 (*j*); 65.23 (*z*); 31.58–22.58 (*k*, *aa* and *an*); 14.02 (*ao*).

3,4,5-Tris[10-(4′-cyanobiphenyl-4-yloxy)decyloxy]benzoic acid 11-[pentakis(4-hexyloxyphenyletynyl)phenoxy] undecyl ester (D1R2)

Synthesis according to the general procedure. Purification using column chromatography (SiO_2, eluent EtOAc:hexane (3:2) to EtOAc:hexane (3:1)) and recrystallisation from CH_2Cl_2:hexane. Yield: 42% of a pale yellow powder. ^{1}H NMR (400 MHz, $CDCl_3$): δ 7.68–7.59 (m, 9H, *H1*, *H2* and *H8*); 7.57–7.44 (m, 15H, *H3*, *H9* and *H17*); 6.94 (dd, 4H, *H4*); 6.86–6.73 (m, 11H, *H10* and *H18*); 4.35 (t, 2H, *H16*); 4.27 (t, 2H, *H14*); 4.04, 4.03, 3.99 and 3.97 (4 × t, 12H, *H7* and *H5*); 3.85–3.84 (3 × s, 15H, *H19*); 1.92–1.25 (m, 50H, *H6* and *H15*). ^{13}C NMR (400 MHz, $CDCl_3$): δ 166.56 (*z*); 159.99, 159.89, 159.80 (*al*); 159.85 (*ac*); 159.73 (*i*); 153.00 (*n*); 148.38 (*m*); 145.20 (*e*); 133.24, 133.10, 133.07 (*aj*); 132.51 (*c*); 131.18, 131.14 (*f*); 128.37 (*ac*); 128.25 (*g*); 126.99 (*d*); 123.82 (*af*); 123.38 (*p*); 122.77 (*q*); 119.83 (*ad*); 119.07 (*a*); 115.69, 115.53, 115.45 (*ai*); 115.00 (*h*); 114.22 (o); 114.09, 114.05 (*ak*); 111.85 (*r*); 109.97, 109.93 (*b*); 99.15, 98.98, 96.91 (*ag*); 86.60, 86.27, 83.54 (*ah*); 74.60 (*ab*); 69.18, 68.92 (*l*); 68.08 (*j*); 67.90 (*z*); 55.30, 55.28 (*am*); 30.56–25.90 (*k* and *aa*).

RESULTS AND DISCUSSION

Synthesis

In order to couple three rods to one single disc, an asymmetric three-to-one linking group is required. We used a gallic acid moiety as the linking and branching group, since it allows the branching to take place within the molecular plane. In addition, it is commercially available and it is readily derivatised by clear-cut etherification and esterification reactions. The synthetic scheme to obtain the linked disc-rod mesogens is drawn in Scheme 1.

Commercially available 4-cyano-4′-hydroxybiphenyl **1** was alkylated with a large excess of α,ω-dibromoalkane, to prevent the formation of large amounts of dimers. The formed dimer was removed from the product by selective recrystallisation and the product **2** or **3** was reacted with ethyl gallate under similar conditions to yield the trimers **R1** and **R2**. In all mixing studies, the trimers **R1** and **R2** were the used materials, since the deprotected analogues **4** and **5** were hard to handle due to their very low solubility in most organic solvents. Subsequent esterification of **4** or **5** with the disc-shaped mesogen **D1** yielded the target compounds **D1R1** and **D1R2** in reasonable to low overall yields. It is noted that, while the catalyst 4-(dimethylamino)pyridine (DMAP) for the latter esterification reaction was activated with *para*-toluene sulphonic acid (*p*TSA), the yields were still unsatisfactory for such esterification reactions.

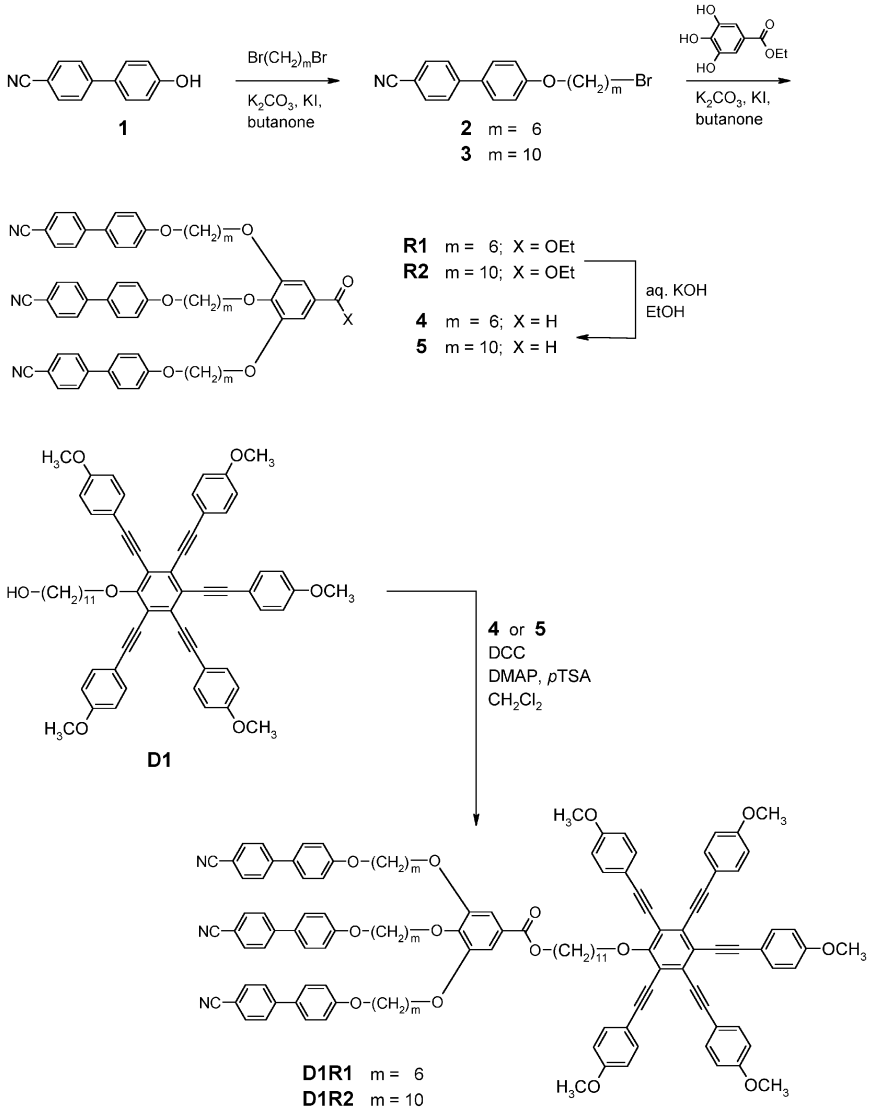

SCHEME 1 Synthesis of the linked disc-rod mesogens.

Liquid Crystalline Properties

The mesomorphic properties of the linked disc-rod mesogens as well as their precursors were investigated by differential scanning calorimetry (DSC) experiments (see Fig. 6) and optical polarising microscopy (OPM) studies (see Figs. 7 and 8). The results are summarised in Table 1.

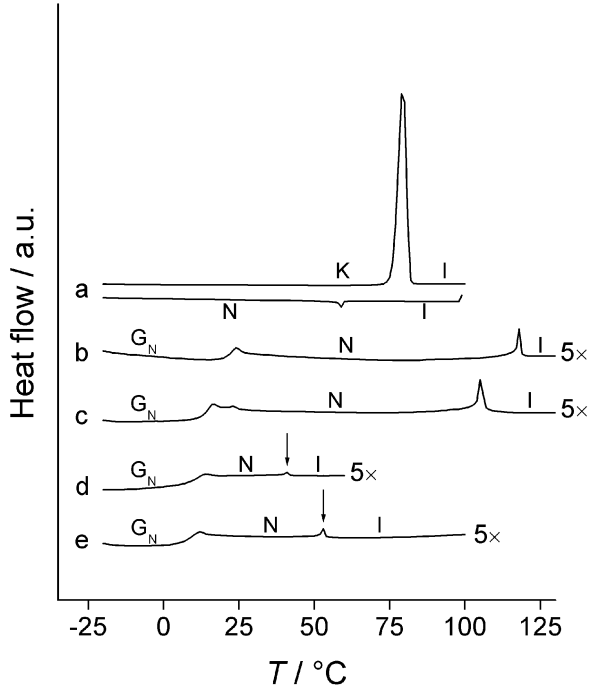

FIGURE 6 Normalised differential scanning calorimetry traces of (a) mesogen **2** (both second heating and cooling curve); (b) short-spacered trimer **R1**; (c) long-spacered trimer **R2**; (d) linked disc-rod mesogens **D1R1** and (e) linked disc-rod mesogen **D1R2**. All heat curves are second heatings. Traces (b) to (e) have been magnified 5 times. The arrows at traces (d) and (e) indicate the small phase transition from the nematic to the isotropic phase.

In the first heating runs, compound **R1** shows a sharp melting peak from crystalline to isotropic at 136°C. Due to supercooling of the crystalline phase (even with low cooling rates), a transition from the isotropic to the nematic phase (see Fig. 7b) was observed at 117°C. Further cooling, did not result in crystallisation and even on annealing at 80°C for an extended period (over a week) no crystallisation was observed. Instead, a glass transition at 21°C was found. The corresponding linked trimer **R2** showed similar behaviour, only the nematic phase (see Fig. 7c) is a common monotropic phase as the crystalline to isotropic transition is observed in the second heating curve as well. The liquid crystalline properties of the disc-shaped mesogen **D1** have been published before [9]. The material shows an enantiotropic nematic mesophase (see Fig. 7d) between the crystalline and the isotropic phase. The linking of the rod-shaped and the disc-shaped species changes the liquid crystalline prop-

TABLE 1 Thermal Properties of the Pure Mesogens. Transition Temperatures [°C] are Determined by DSC as well as OPM. Latent Heat Values (between the brackets) are Given in [J g^{-1}].

Mesogen	Phase behaviour						
D1[a]	K	71 (33)			N	118 (0.2)	I
R1[b]	G_N	21			N	117 (1.5)	I
R2[c]	K	[69 (60)	N	105 (6.1)]		119 (104)	I
D1R1	G_N	10			N	41 (0.2)	I
D1R2	G_N	8			N	52 (0.5)	I

[a]The mesomorphic properties of **D1** have been described before [7].

[b]The mesophases of **R1** is monotropic, however after the first heating run (melting peak: $T_m = 136°C$, $\Delta H = 81.4\,J\,g^{-1}$), the samples do not show any sign of crystallisation during cooling, nor during subsequent heating runs. Even upon extensive annealing (> 24 hrs at 80°C), no crystallisation was observed.

[c]Compound **R2** shows a common monotropic phase.

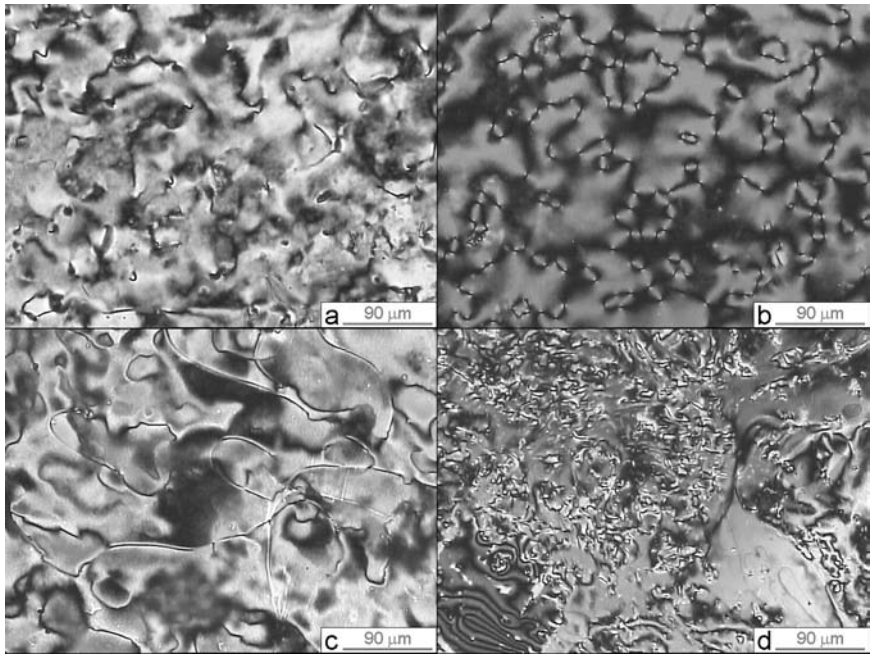

FIGURE 7 Optical polarising microscope photographs of the starting materials: (a) the nematic phase of short-spacered cyanobiphenyl **2** at 50°C; (b) the nematic phase of the short-spacered trimer **R1** at 110°C; (c) the nematic phase of the long-spacered trimer **R2** at 110°C and (d) the nematic phase of the disc-shaped mesogen **D1** at 80°C. All pictures are taken with crossed polarisers. The bar shown in the photographs has a length of 90 µm. (See Color Plate I).

erties drastically. In both linked disc-rod materials a nematic mesophase is observed with a grainy texture which was impossible to identify (see Fig. 8a). Only in thin areas, a schlieren texture could be observed, indicative of a nematic order (see Fig. 8b). After extensive annealing, we were able to grow larger domains and it was found that the mesogens align homogeneously, see Figures 8c and 8d. The clearing temperatures, however, were reduced significantly with respect to the individual constituents. Besides, in these materials crystallisation is fully suppressed and the materials show a glass transition at low temperatures. The DSC traces of the disc-rod mesogens show a nematic to isotropic phase transition with a small latent heat, characteristic for such transitions found for these disc-shaped mesogens.

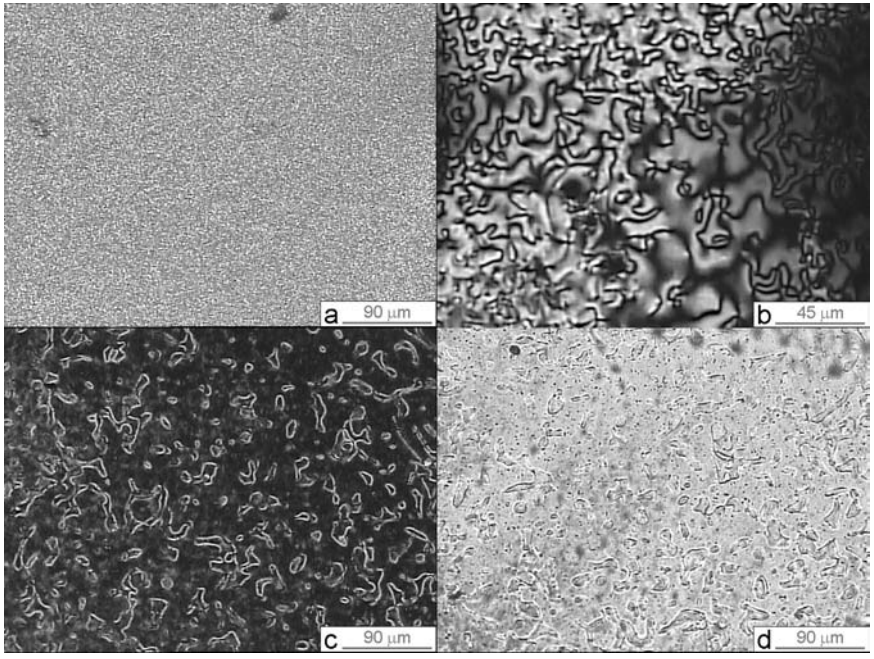

FIGURE 8 Optical polarising microscope photographs of the linked disc-rod mesogens **D1R1** and **D1R2**: (a) the grainy texture of a freshly formed nematic phase of **D1R1** at 39°C; (b) the *schlieren* texture of a freshly formed nematic phase **D1R2** at 50°C; (c) and (d) aligned textures (director of the nematic phase parallel to the substrates) obtained by annealing the sample 24 hours at 50°C between unprepared microscope slides: (c) shows low birefringence (**n** ∥ to the analyser or polariser) and (d) shows a high birefringence (**n** with an angle of ± 45° with respect to the analyser). All pictures are taken with crossed polarisers. The bar shown in the photographs (a), (c) and (d) has a length of 90 μm; in (b) a length of 45 μm. (See Color Plate II).

The nature of the observed nematic phases (whether they are uniaxial or biaxial and whether their birefringence is positive or negative) is subject to further study in the near future.

Mixing Studies

Since simple mixture of rods and discs show macroscopic phase separation, we studied the mixing behaviour of our linked disc-rod mesogens with their appropriate constituents. In order to investigate the mixture over a full composition range, contact samples were prepared. As a reference experiment, a contact sample between of the disc-shaped mesogen **D1** and the rod-trimer **R1** was made as well, see Figure 9. Both materials mix in the

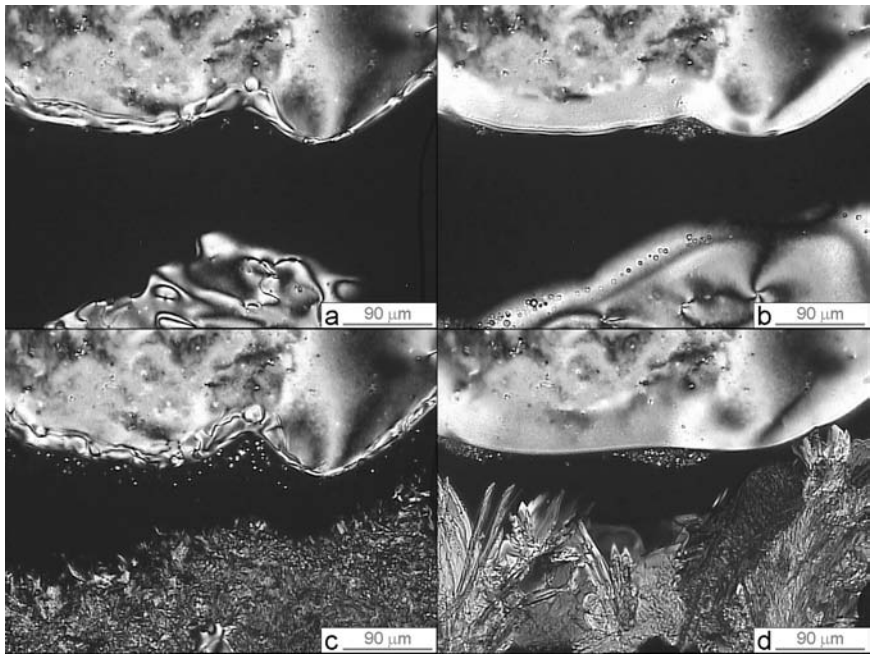

FIGURE 9 Optical polarising microscopy studies of a contact sample of **R1** (top) and **D1** (bottom) on cooling. Both materials are miscible in the isotropic phase. The pictures show various stages of the cooling run: (a) and (b) 70°C and 60°C (both materials nematic, separated by an isotropic region; (c) 50°C (**D1** starts crystallising, the isotropic region is still clearly visible); (d) Room temperature (the isotropic phase between the crystals of **D1** and the glass of **R1** is still present. All pictures are taken with crossed polarisers. The bar shown in the photographs has a length of 90 μm. (See Color Plate III).

isotropic phase, i.e. at high temperatures no macroscopic phase separation could be observed. Cooling the contact sample results in the formation of the nematic phase of both pure materials at their clearing temperatures, leaving an isotropic mixing region in the middle of the sample (see Fig. 9a). Further cooling results in a shift of the phase boundaries towards the centre of the sample (Fig. 9b), indicating a slight solubility of one material in the other, however, strongly destabilising the mesophase. When the sample is cooled to room temperature (Fig. 9d), the discs **D1** have crystallised and the nematic phase of the rods **R1** is frozen into a glassy state. However, in the middle of the sample, the isotropic region is still clearly visible. This behaviour was anticipated based on the results of previously reported experiments.

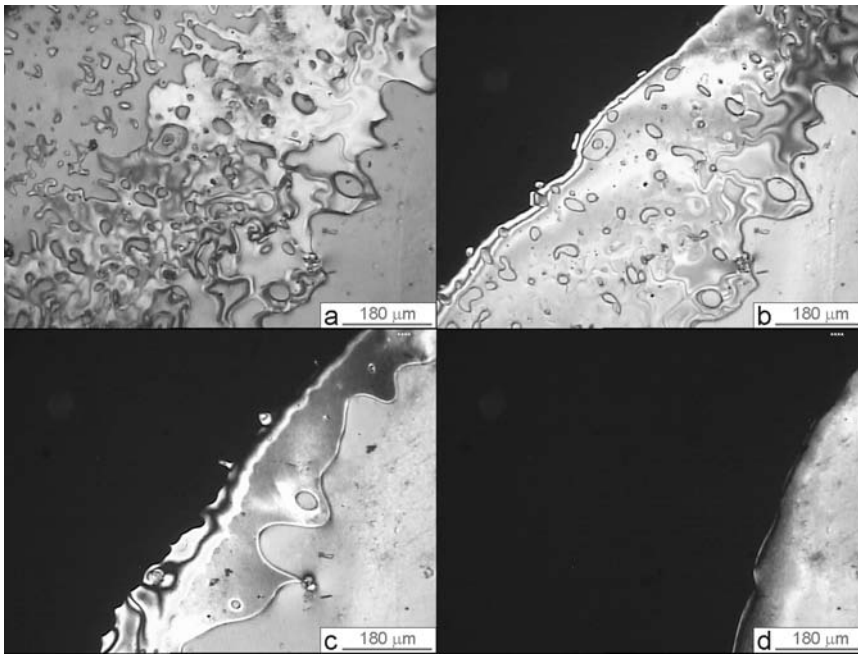

FIGURE 10 Optical polarising microscopy studies of a contact sample of **D1R1** (left) and **R1** (right) on heating. Before the experiment, the contact sample was annealed for 16 hours at 40°C. The pictures show various stages of the heating run: (a) 40°C (just below the clearing temperature of **D1R1**); (b) 65°C; (c) 100°C and (d) 115°C (just below the clearing temperature of **R1**). The nematic to isotropic transition slowly shifts from left to right, indicating a linear miscibility between the two mesogens. All pictures are taken with crossed polarisers. The bar shown in the photographs has a length of 180 μm. (See Color Plate IV).

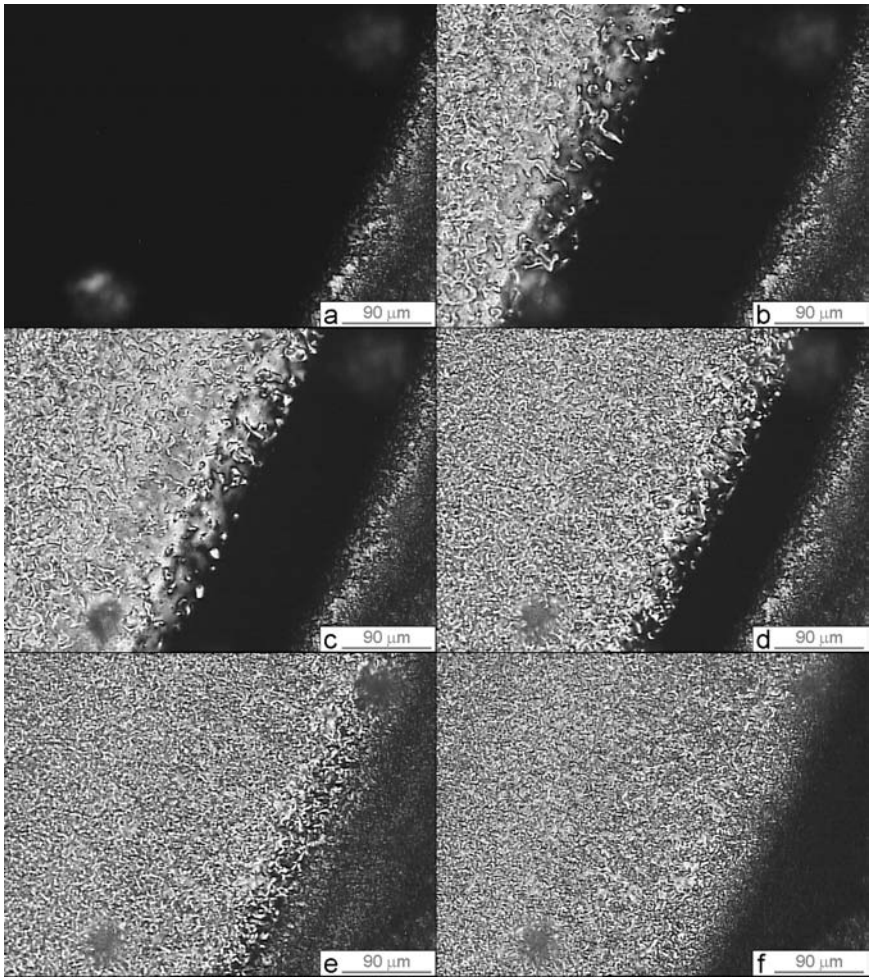

FIGURE 11 Optical polarising microscopy studies of a contact sample of **D1R2** (left) and **D1** (right) on cooling. The pictures show various stages of the cooling run: (a) 54°C (super-cooled nematic phase of **D1** in bottom right corner); (b) 50°C (nematic phase of **D1R2** sets in at the opposite corner); (c) 46°C, (d) 42°C and (e) 38°C (nematic phases of **D1R2** and **D1** (at the fringes, as the bulk has crystallised) slowly grow together and meet at 38°C); (f) after annealing for 30 minutes at 30°C: both nematic phases are homogeneously mixed now. The bar shown in the photographs has a length of 90 µm. (See Color Plate V).

The disc-rod mesogen **D1R1** and the trimer **R1** showed a linear mixing behaviour between the clearing temperatures of both constituents ($T_{NI,\mathbf{R1}} = 117°C$ and $T_{NI,\mathbf{D1R1}} = 41°C$). Four frames from a motion picture of a cooling experiments (cooling rate 5°C min^{-1}) were selected and shown in Figure 10.

Neither of the mixtures of **D1** with **D1R1** and **D1** with **D1R2** showed linear mixing behaviour. At temperatures below the clearing temperatures of both individual constituents, the mixture remained isotropic over a wide concentration range, as observed in Figure 11b. Cooling (typical cooling rate of 2–5°C min^{-1}) the contact samples results in a shift of the two nematic to isotropic interfaces towards each other, until both meet at ~24°C for the materials with **D1R1** and 38°C for the materials with **D1R2**. On annealing at this temperature [8] a homogeneously mixed system is obtained, wherein no phase boundaries could be observed (see Fig. 11f).

To the best of our knowledge, **D1R1** and **D1R2** are the first materials that bridge the gap between rod-shaped and disc-shaped liquid crystals by showing an enantiotropic nematic phase by itself *and* its nematic phase being miscible with both rod-shaped and disc-shaped mesogens, the latter two showing no mutual miscibility.

CONCLUSIONS

We have prepared two novel mesogens built-up from disc-shaped and rod-shaped mesogens. By attaching three rods to one single disc, the weight (and volume) fractions of both constituents are roughly matching. Both of the linked disc-rod mesogens show a nematic mesophase. No trace of the nanophase separation between the disc and the rods, resulting in layered mesophases could be detected. Mixing experiments of **R1** with **D1R1** show linear mixing behaviour over the entire composition range. Mixtures of **D1R1** or **D1R2** with **D1** show an apparent minimum in the middle of the phase diagram. However, results form optical microscopy studies clearly indicate that at temperatures below the lowest clearing point a nematic phase is formed from the homogeneously mixed compounds. We believe that this is the first series of materials that actually shows a continuous nematic phase in between the two extremes, that are set by the rods (with a positive birefringence) and the discs (with a negative birefringence). Construction of a proper phase diagram, measurements of the birefringence along the composition range as well as verification of the symmetry of the nematic phase are in full progress and will be reported shortly.

REFERENCES

[1] The 25th anniversary of discotic liquid crystals is set by the important 1977 publication: Chandrasekhar, S., Sadashiva, B. K., & Suresh, K. A. (1977). *Pramana*, *9*, 471.

[2] (a) For a review on chemical structures of discotic liquid crystals read: Cammidge, A. N. & Bushby, R. J. (1998). In: *Discotic Liquid Crystals: Synthesis and Structural Features*, Demus, D., Goodby, J. W., Gray, G. W., Spiess, H. W., & Vill, V. (Eds.), Wiley VCH: New York, Vol. 2B, 693–748.
(b) For e review on discotic liquid crystals showing a nematic mesophase read: Praefcke, K. (2001). In: *Physical Properties of Liquid Crystals: Nematics*, Dunmur, D. A., Fukuda, A., & Luckhurst, G. R. (Eds.), INSPEC: London, 17–35.

[3] (a) Vanakaras, A. G., McGrother, S. J., Jackson, G., & Photinos, D. J. (1998). *Mol. Cryst. Liq. Cryst.*, *323*, 199.
(b)Sharma, S. R., Palffy-Muhoray, P., Bergersen, B., & Dunmur, D. A. (1985). *Phys. Rev. A*, *32*, 3572.

[4] (a) Palffy-Muhoray, P., de Bruyn, J. R., & Dunmur, D. A. (1985). *J. Chem. Phys.*, *82*, 5294.
(b) Pratibha, R. & Madhusudana, N. V. (1985). *Mol. Cryst. Liq. Cryst. Lett.*, *1*, 111.
(c) Hashim, R., Luckhurst, G. R., Prata, F., & Romano, S. (1993). *Liq. Cryst.*, *15*, 283.

[5] (a) Fletcher, I. D. & Luckhurst, G. R. (1995). *Liq. Cryst.*, *18*, 175–183.
(b) Hunt, J. J., Date, R. W., Timimi, B. A., Luckhurst, G. R., & Bruce, D. W. (2001). *J. Am. Chem. Soc.*, *123*, 10115–10116.

[6] The molecular weight of pentakis(4-methoxyphenylethynyl)phenoxy core is about three times the molecular weight of the cyanobiphenyl core.

[7] (a) Kouwer, P. H. J., Jager, W. J., Mijs, W. F, & Picken, S. J. (2002). *Macromolecules*, *35*, 4322–4329.
(b) Kouwer, P. H. J., Jager, W. F., Mijs, W. J., & Picken, S. J. *submitted to J. Mater. Chem.*

[8] Annealing was carried out typically for 30 minutes to two hours just below the lowest observed clearing temperature in the phase diagram. Annealing was necessary to allow phase formation and domain growth, as the viscosity of the linked disc-rod mesogens is rather high at such temperatures.